Exp. Theo. NANOTECHNOLOGY 10 (2026) 611-625 https://doi.org/10.56053/10.2.611

Simulation using high-power lc arc plasma for diagnosing plasma parameters and nanoparticle formation from a meteorite sample

Omar Al-Juboori[*], *Waleed Ibrahim Yaseen, Hussein Omran Hussein, Duraid A. Al-Shakarchi, Haider K. Ahmed*

Department of Astronomy and Space, College of Science, University of Baghdad, Baghdad, Iraq
[*]) Email: omar.t@sc.uobaghdad.edu.iq

Received 13/2/2026, *Received in revised form* 19/3/2026, *Accepted* 30/3/2026, *Published* 15/4/2026

Meteorite classification is fundamental to understanding their geochemical and mineralogical composition. This study explores a novel approach to classification by analyzing the spectral emission ratios of key elements generated from the plasma formed around meteorites. When entering Earth's atmosphere meteorites experience extreme thermal and mechanical stress due to high-velocity air resistance leading to plasma formation and fragmentation. To reproduce such conditions a high-power LC-type device is introduced here for the first time to generate plasma in a controlled laboratory environment. Using a power output of up to 300 watts this device enabled the ablation of a real meteorite target in a vacuum chamber producing plasma spectra under low-pressure conditions (1–4 mbar) and a power input of 2000 watts. The study examined Fe I emission lines at wavelengths of 526.9, 532.8, 537.1, 539.7, 540.5, 542.9, and 543.4 nm. Using the Boltzmann plot method and Stark broadening analysis the plasma parameters including temperature and electron number density are determined. This work introduces a promising technique for enhancing meteorite classification through controlled plasma spectroscopy. Additionally, the ablation of the meteorite surface under high-energy plasma conditions is examined as a possible mechanism for nanoparticle formation.

Keywords: High-power; OES technique; Plasma; Chondrite; Nanoparticle.

1. INTRODUCTION

The study of meteorites is crucial especially due to their close connection with asteroids and their interactions with Earth [1,2]. Analysis of meteorites and asteroid fragments that reach Earth can provide insights about the origins of meteorites and their connection to asteroids [3]. Effective techniques for reducing the risks posed by meteorite impacts like the well-known Chelyabinsk event, require a deep understanding of meteorite impacts basic behavior and dynamics [4]. When the meteorite passes through Earth's atmosphere it experiences a braking force that generates a shock wave. This interaction leads to the loss of part of the meteorite's mass a process commonly known as disintegration [5]. Shock waves generated by its deceleration raise their temperature and form a plasma cloud. During this process molecular and atomic spectral emissions are produced at various stages of the meteor's entry [6]. Metals particularly iron play a fundamental role in the composition of meteorites [7]. Iron exists either in pure form or as part of an alloy and is commonly found in iron meteorites and chondrites [8]. The plasma cloud surrounding the meteor contains prominent spectral lines of neutral iron and iron oxides typically the dominant species present [9]. While the surrounding plasma keeps a relatively lower temperature usually between 3000 and 4000 Kelvin [10] the meteor's core can reach temperatures of up to 95000 Kelvin [11]. The meteorite's atomic and molecular species are sufficiently excited by this temperature environment to produce spectral lines particularly those associated with iron and iron oxide that are clearly visible. Can be also observe the appearance of lines for magnesium Mg calcium Ca aluminum Al and their oxides within the spectral range of 450 to 600 nanometers which is consistent with the Benichoff meteorite [12]. The phenomena associated with meteoroid entry into Earth's atmosphere can be simulated using cold plasma at atmospheric pressure [13] and Laser-Induced Breakdown Spectroscopy (LIBS) technique [14]. This method enables the comparison between laboratory-generated spectra and those obtained from actual meteorites [10] high-temperature plasma systems [3] or arc heaters [15]. Popov and others used pulsed lasers to simulate the entry of meteorites into Earth's atmosphere and analyze the spectra in the laboratory. They found that the electron temperature ranged from 0.2 to 4 electron volts and the electron density is between 10^{14} and 10^{19} cm^{-3}. This result demonstrates that this technique is very suitable for studying meteorites. This technique allows for pressure variations when using vacuum systems which simulates the altitudes at which meteorites disintegrate in nature and produces spectral emissions identical to those found in nature [16]. The state in which the negative charge of the ions and the positive charge of the ions are approximately equal i.e. electrically neutral is called the state of plasma with the presence of neutral atoms [17]. Plasma can also be defined as a partially ionized gas found in nature and also generated in the laboratory. It has numerous applications across various industrial and medical fields including surface treatment and determining the chemical composition of synthetic and natural materials [15] [18]. Several analytical methods are commonly employed in laboratories to investigate the composition of meteorites including Energy Dispersive Spectroscopy [19] Inductively coupled plasma mass spectrometry and X-ray Fluorescence [20]. A practical and effective approach to studying the elemental composition of meteorites during atmospheric entry is through the spectral analysis of the plasma emissions generated around them [21]. Thermodynamic equilibrium must be assumed to implement this method for plasma diagnosis and to calculate electron temperature and electron density using the Boltzmann method and Stark expansion respectively [22]. In this study an LC-type power supply is used to generate high-energy electrical discharges producing intense heat around a chondrite meteorite model. This thermal setting caused plasma to form around the target simulating conditions like those during atmospheric entry. The high energy input caused the meteorite to partially fragment and emit spectral lines which are recorded using spectrometric techniques. In addition, the ablation of the meteorite surface under high-energy plasma conditions is examined as a potential mechanism for nanoparticle formation. This combined research helps improve understanding of plasma diagnostics plasma matter interactions and nanoparticle generation processes associated with meteorite materials.

2. PLASMA DIAGNOSTICS

An LC device is used to generate high-energy electrical discharge plasma to generate plasma around the meteorite sample used in this work. For plasma characterization the Boltzmann method is used to calculate the electron temperature (T_e) and the Stark expansion method to calculate the electron density (n_e) [23]. These methods are chosen due to their high reliability in laboratory plasma characterization. Based on previous studies by Huddleston and Leonard [22] and Cristoforetti et al. [2] the existence of thermodynamic equilibrium for the plasma should be assumed. High melting point tungsten electrodes are used and the meteorite sample is mounted on one of the electrodes. The system is powered using a high-energy LC at a variable operating pressure. Plasma light emissions are collected through a lens system and transmitted to the spectrometer via an optical fiber. Due to the high energy involved in the arc discharge the plasma spectra are intense and clear emission lines of the elements ablated from the meteorite sample are observed. These emissions result from the excitation and ionization of the materials evaporated from the meteorite at high temperatures. The T_e is calculated using the Boltzmann plot method based on the following relation [24]:

$$\ln\left(\frac{\lambda I}{A_{ki}g_k}\right) = C - \frac{E_k}{kT_e} \tag{1}$$

In the above relation I is the relative intensity of the emission line λ is the wavelength A_k is the transition probability g_k is the statistical weight of the upper energy level k and E_k is the energy of that level. The constants k and T_e represent the Boltzmann constant and the electron temperature respectively. In this experiment C is a constant. Electric fields generated by fast-moving electrons and comparatively slower ions in the plasma lead to shifts in the energy levels of atoms and ions. This interaction results in the broadening of the spectral emission lines a phenomenon known as Stark broadening. The electron density (n_e) of the plasma can be determined from the spectral line width associated with the Stark broadening. Specifically the n_e is proportional to the full width at half maximum of the Stark-broadened spectral line and this relationship can be expressed as [25]:

$$\Delta\lambda_{1/2} = 2\omega\left(\frac{n_e}{10^{16}}\right) \tag{2}$$

Here ω represents the electron impact width variable and n_e is the electron density (in cm^{-3}). The impact component values are obtained from [26]. The interaction of charged particles in a plasma leads to the reduction of the local electric field effects a phenomenon known as Debye shielding (λ_D) which is given by [27]:

$$\lambda_D = \left(\frac{\varepsilon_o kT_e}{n_e e^2}\right)^{1/2} \tag{3}$$

One of the fundamental conditions for a gas to be considered a plasma is that λ_D should be much smaller than the characteristic dimension of the system L (in cm), i.e. $\lambda_D << L$. where e is the electron charge ε_o is the permittivity of free space and k is Boltzmann's constant [28]. The Plasma frequency can be calculated using the following [29]:

$$\omega_p = \sqrt{\frac{n_e e^2}{\varepsilon_o m_e}} \tag{4}$$

where m_e is the mass of the electron.

3. EXPERIMENTAL DETAILS

A vacuum system is employed to generate plasma around a meteorite model under controlled conditions. The setup consists of a cylindrical glass chamber with a length of 30 cm, an internal diameter of 20 cm, and a wall thickness of 0.5 cm. A resistive iron base supports the internal components, including the electrodes, gas inlet, and air outlet for discharge operations. Steel electrodes are selected to prevent contamination from electrode material evaporation during plasma generation. The meteorite model is mounted as a target on one of the electrodes. The chamber is evacuated using a two-stage rotary vacuum pump, achieving a base pressure of approximately 0.1 mbar. Figure 1 illustrates the schematic of the vacuum system, including all the essential components and the attached instrumentation used during the plasma generation and diagnostics.

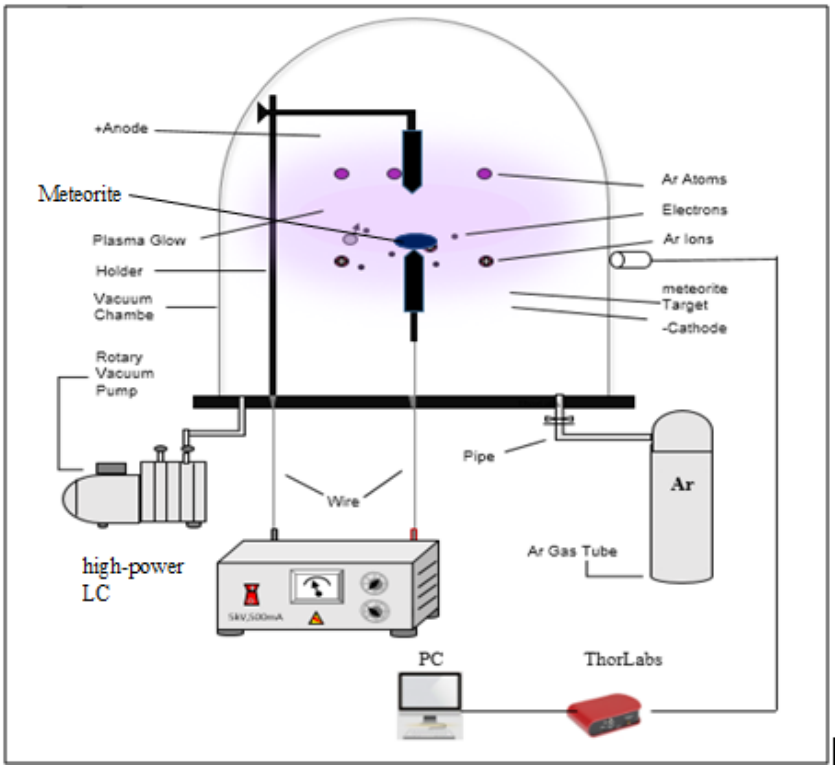

Figure 1 Vacuum system.

A high-power supply is employed, operating on the principle of resonance between a capacitor and an inductor coil. This resonance enables the generation of the high current necessary for producing the arc plasma between the electrodes within the vacuum chamber. The device can deliver up to 2000 watts of power, making it suitable for a wide range of plasma-related applications. To operate the power supply, a voltage of approximately 300 volts is applied. Upon activation, the voltage rises to approximately 1000 volts due to the presence of a capacitor and an inductor inside the device, generating resonance that increases the voltage. During plasma generation, the voltage drops while the current increases significantly, generating an electric arc plasma. This plasma interacts with the meteorite sample, causing fragmentation and vaporization of a portion of the sample, and the formation of nanoparticles after cooling at the end of the experiment. This resulted in the formation of a plasma cloud containing ionized gas and vaporized meteorite fragments. The emission spectra from this plasma are prominent and captured using a spectrometer. Light emitted from the plasma is collected through a lens and delivered to the spectrometer via an optical fiber for analysis.

4. RESULTS AND DISCUSSION

Plasma is successfully generated around the meteorite model inside the vacuum chamber using a 2000-watt high-power LC power supply with experiments conducted at varying pressures of 1, 2, 3, and 4 mbar, as illustrated in Figure 2.

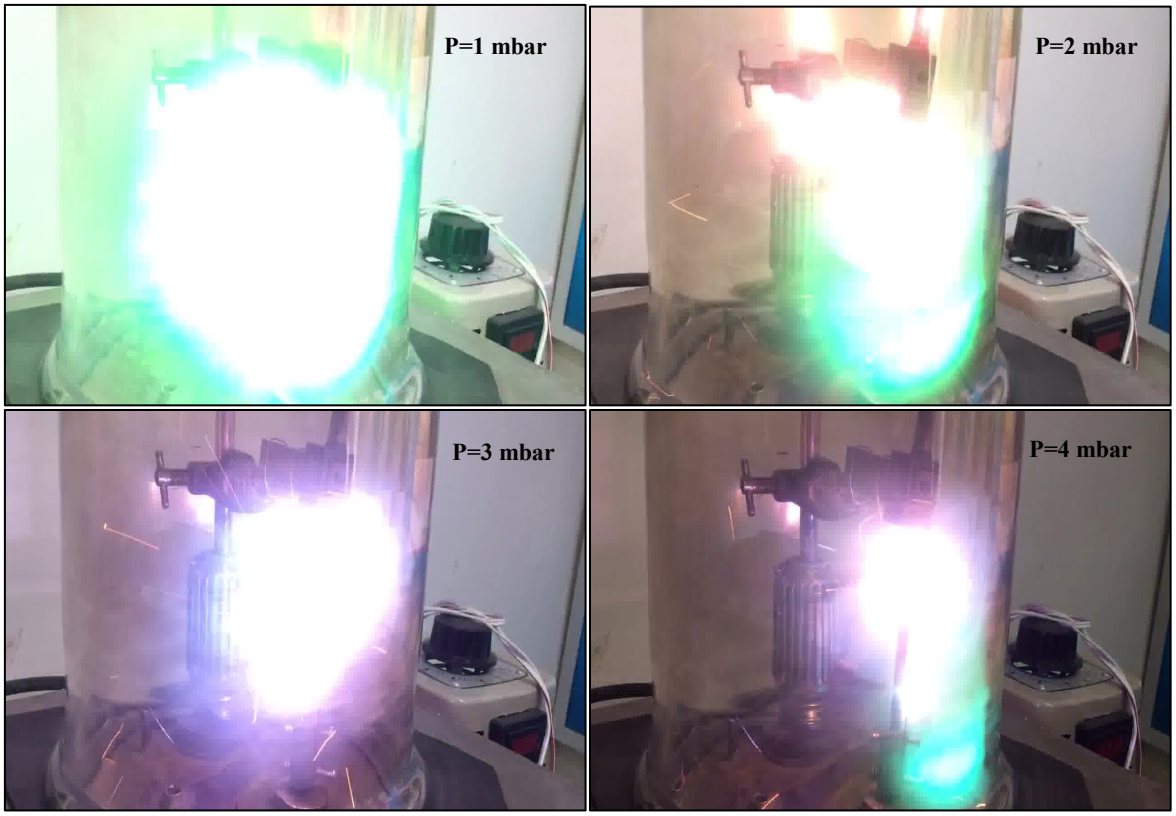

Figure 2 Glow LC Arc plasma LC for the model meteorite.

To diagnose the plasma and determine key parameters such as T_e and n_e the emission spectrum of neutral iron (Fe I) is recorded using a spectrometer, as shown in Figure 3. The plasma is assumed to be in a state of local thermodynamic equilibrium to facilitate accurate diagnostics. The Fe I emission lines used in the analysis are observed at the following wavelengths: 526.97, 532.89, 537.10, 539.71, 540.53, 542.97, 543.45, 544.69, and 545.56 nm [28-33]. The spectroscopic parameters for these transitions are obtained from the NIST Atomic Spectra Database and are summarized in Table 1.

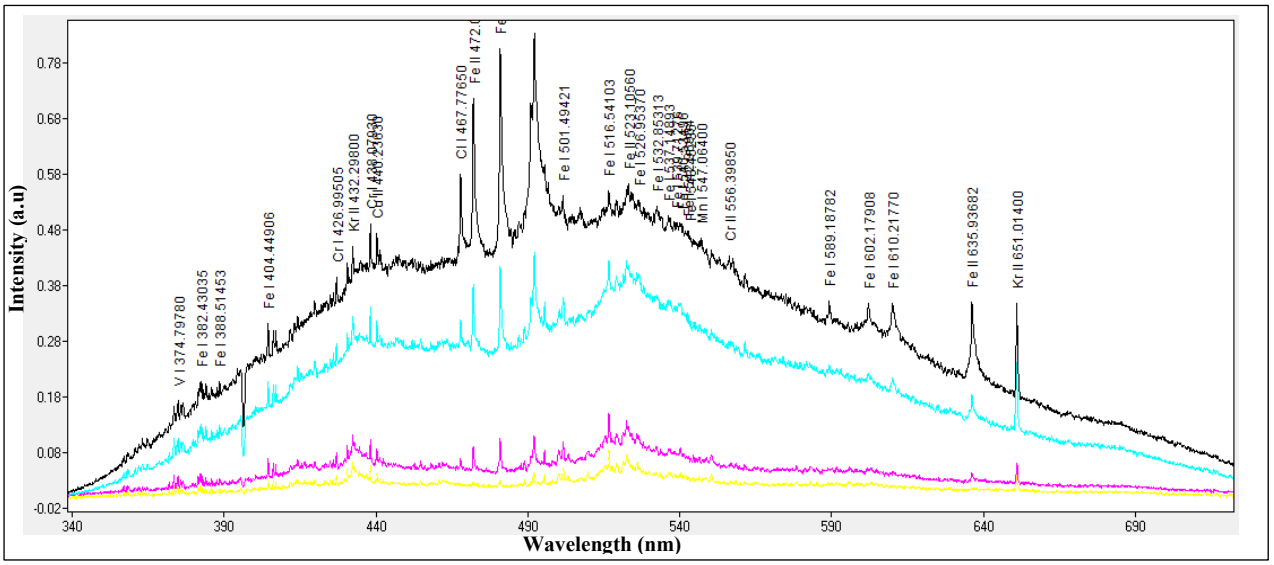

Figure 3 Emission spectrum of the meteorite chondrite.

Table 1 Parameters of the spectrum for Fe I obtained from the NIST database.

FeI Wavelength (nm)	Ag	E_i (eV)	E_k (eV)	Fe I Intensity
507.973	1.56e+05	0.99011115	3.43018998	0.833
526.97	1.14e+07	0.85899575	3.21118938	0.523
537.10	5.25e+06	0.95815732	3.26570610	0.489
540.53	3.27e+06	0.99011115	3.28302483	0.475
542.97	2.99e+06	0.95815732	3.24096914	0.473
543.45	1.70e+06	1.01105568	3.29183986	0.466
544.69	2.74e+06	0.99011115	3.26570610	0.460
545.56	1.82e+06	1.01105568	3.28302483	0.453

Figure 4 presents the variation in the peak intensities for the selected Fe I lines at 526.97, 532.89, 537.10, 539.71, 540.53, 542.97, and 543.45 nm. The figure demonstrates that all emission lines exhibit a systematic decrease in intensity with increasing pressure. Naturally, the emission intensities of the excited species generated in the plasma are influenced by several factors, most notably the applied voltage and the flow velocity of the working gas, whether in a static environment or a flowing medium [34-36].

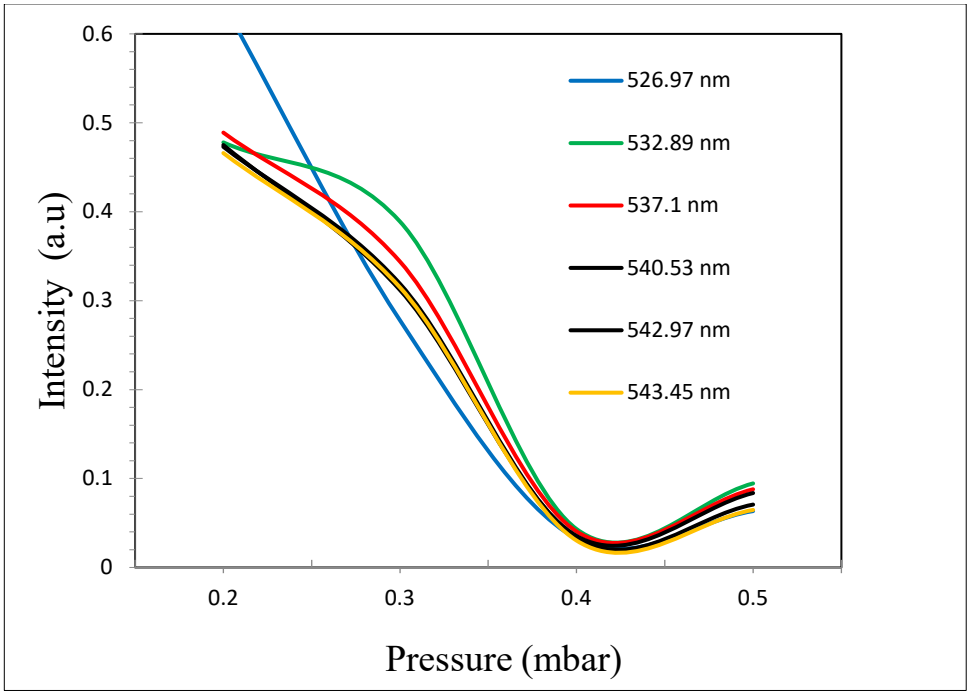

Figure 4 Variation in peak intensities for selected Fe I lines at the above wavelengths (nm) with pressure.

The T_e is calculated using the Boltzmann plot method by Equation (1) using the spectroscopic data provided in Table 1. By plotting Ln (I λ/hcgA) versus the upper energy level E_i, a linear relationship is obtained where the inverse of the slope of the best-fit line corresponds to the T_e as displayed in Figure 5.

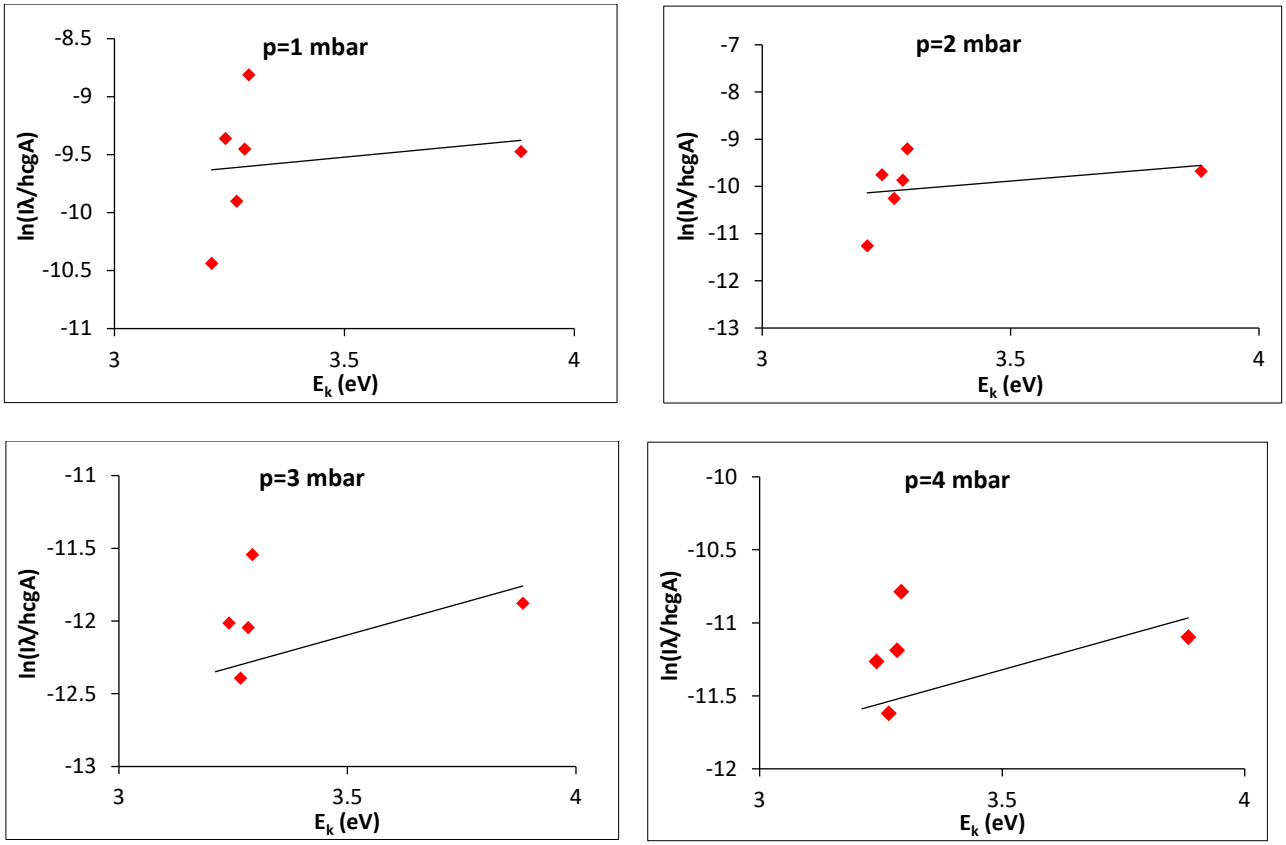

Figure 5 Boltzmann plots of FeI with different pressures, 1, 2, 3, and 4 mbar.

This method requires that the selected emission lines originate from the same atomic species (in this case, Fe I) and all relevant transition data including wavelength statistical weight and transition probability are obtained from the NIST to ensure accuracy [37-40]. From Figure 6 can be observe the relationship between electron temperature and pressure where the electron temperature decreases from 1.19 to 1.07 eV when the pressure values increase from 1 to 4 mbar [41-45]. This is due to the high heat exchange between the molecules because of the increase in their numbers. Figure 7 displays the spectral line at 526.97 nm where the Lorentzian fitting is applied to determine the full width at half maximum ($\Delta\lambda$). This width is then used to estimate the n_e at various pressures using the Stark broadening method based on the typical impact broadening values for this line. According to Eq. (2) ω is taken as 0.011 nm for the peak λ=526.97 nm Fe I line [46-50]. At pressures of 1, 2, 3, and 4 mbar the measured full widths at half maximum ($\Delta\lambda$) are 210.03, 207.00, 205.49, and 199.75 nm respectively. It is also observed that the peak intensity increased with pressure indicating an enhancement in the Fe I species emission within the LC high-power plasma environment surrounding the meteorite model [51-55].

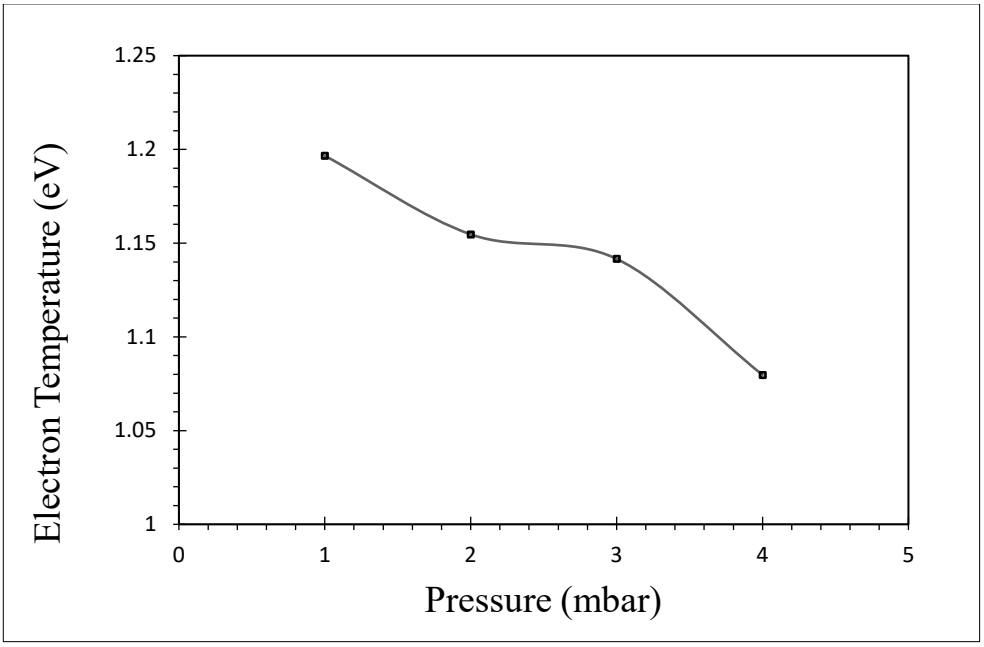

Figure 6 Variation of T_e with pressure.

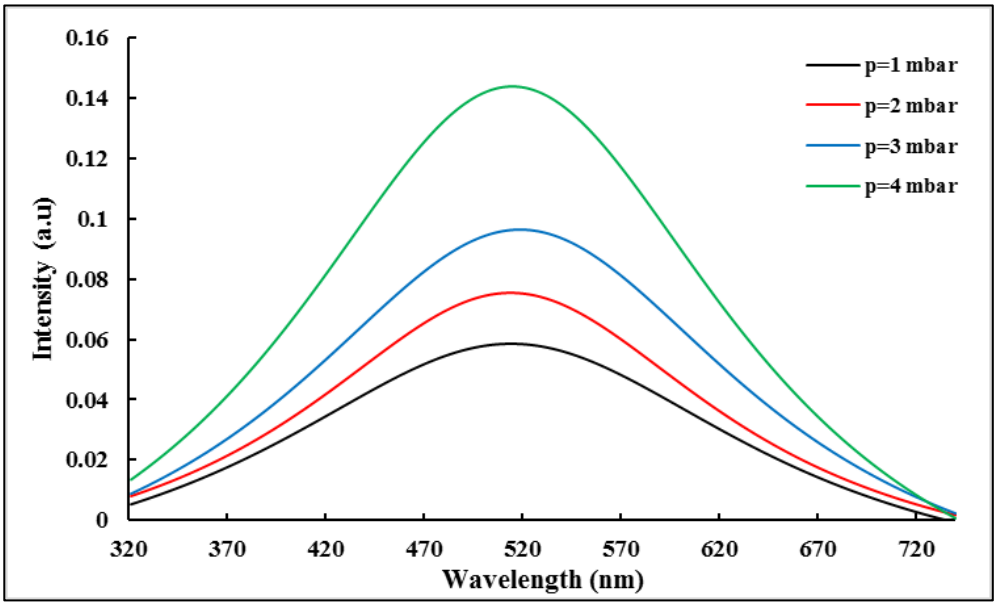

Figure 7 Broadening of the 493.5 nm peak and its Lorentzian fitting at various pressures.

Figure 8 presents the variation of n_e as a function of the gas pressure [56-60]. The results indicate that n_e increases with rising pressure, which is attributed to the enhanced ionization processes occurring within the plasma at higher gas densities [61-65]. This behavior is consistent with the findings reported in [29].

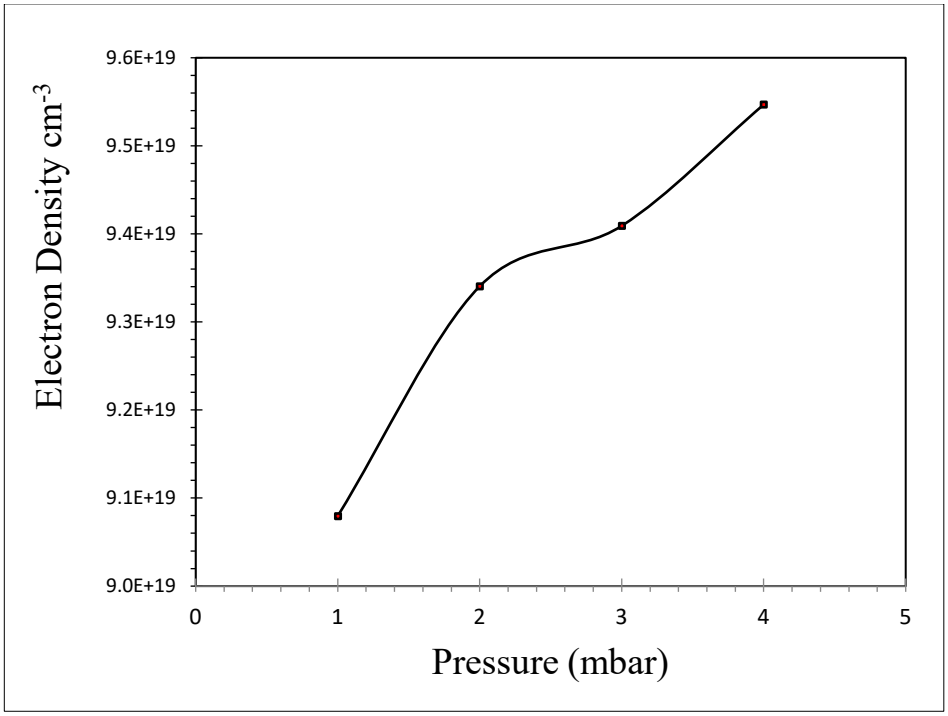

Figure 8 Variation of n_e with pressure.

Pressure is a crucial factor influencing plasma generation in vacuum systems. As pressure increases the number of gas atoms within the plasma generating chamber increases leading to more collisions between gas molecules and greater heat exchange [66-70]. This results in a decrease in electron temperature and an increase in electron density. Pressure is used as a variable to study the plasma generated around a meteorite sample when determining the plasma parameters (T_e) and (n_e). Four different pressure values are used 1, 2, 3, and 4 mbar corresponding to altitudes of 32, 30, 29.5, and 28.8 km respectively using pressure to altitude conversions based on a standard atmospheric model [71-75]. These altitude values represent the altitudes at which the meteorite would naturally disintegrate and erode upon entering Earth's atmosphere. According to Equation (3) the Debye length is directly proportional to the T_e and inversely proportional to the n_e. As shown in Figure 9 the Debye length decreases with increasing gas pressure. This trend is attributed to the concurrent decrease in T_e and increase in n_e, both of which are pressure dependent parameters influenced by the input power and collisional processes in the plasma [76-80]. Additionally Figure 9 also demonstrates the relationship between the plasma frequency and the working pressure. It is evident that plasma frequency increases with increasing pressure a behavior that directly follows the trend of rising n_e as described by Equation (4). These results are consistent with the previous findings reported in [30].

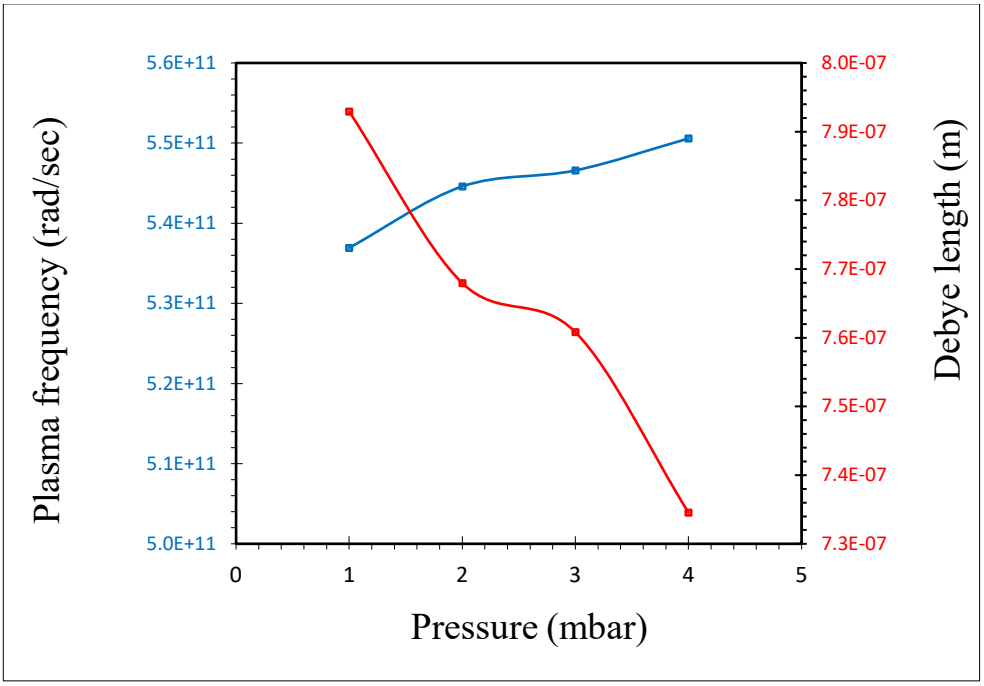

Figure 9 Variation of Debye length and plasma frequency as a function of pressure.

In addition to spectral emission phenomena the interaction between high energy plasma and the meteorite surface can lead to the formation of nanoparticles. During the ablation process atoms ions and small clusters are ejected from the meteorite surface and expand into the surrounding plasma environment forming a dense plasma plume. As this plume expands and cools rapidly the vaporized species may undergo nucleation and condensation processes [81-84].

5. CONCLUSIONS

This study demonstrated the generation and diagnostic analysis of plasma formed around a chondrite meteorite model using a high-power LC arc discharge system under controlled vacuum conditions, which was utilized for the first time globally in the classification of meteorites. When comparing the LC device to a pulsed laser it surpasses the laser in terms of generating plasma for extended operating periods making it ideal for meteorite fragmentation. Its power reaches up to 2000 watts continuously and uninterrupted during the experiment. Atomic iron (FeI) lines were used to characterize the plasma and calculate its parameters using the Boltzmann method and the Stark expansion method. The results showed agreement with previously published data encouraging the use of this method for studying meteorites and simulating real world meteorite conditions. This study demonstrated that high-energy generation using an L-C device is a reliable precise and controllable alternative to pulsed lasers for meteoroid research and plasma generation. This facilitates numerous studies on meteoroids including classification and chemical composition analysis using optical emission spectroscopy which helps in understanding their behavior within Earth's atmosphere. Pressure within the vacuum chamber was used as a function of plasma parameters to simulate the altitude at which meteoroids descend. Specific pressure values of 1, 2, 3, and 4 mbar were used corresponding to altitudes of 32, 30, 29.5, and 28.8 kilometers respectively. When a meteorite sample is exposed to high energy using an LC device in addition to the generation of plasma its material ionizes disintegrates and crystallizes forming nanoparticles when cooled. This process explains the interaction between the meteorite material and

the generated plasma and provides a deeper understanding of the ablation processes that occur to meteorites when exposed to high energy.

References

[1] A.S. Zakuskin, B.G. Beglaryan, T.A. Labutin, Astron. Astrophys. 670 (2023) 13 https://doi.org/10.1051/0004-6361/202245462
[2] G. Cristoforetti, S. Legnaioli, V. Palleschi, A. Salvetti, E. Tognoni, Spectrochim. Acta Part B At. Spectrosc. 59 (2004) 1907 https://doi.org/10.1016/j.sab.2004.09.003
[3] A. Drouard, P. Vernazza, S. Loehle, J. Gattacceca, J. Vaubaillon, B. Zanda, Astron. Astrophys. 613 (2018) 54 https://doi.org/10.1051/0004-6361/201732225
[4] O.P. Popova, P. Jenniskens, V. Emel'yanenko, A. Kartashova, A. Biryukov, Biryukov, Science 342 (2013) 1069 https://doi.org/10.1126/science.1242642
[5] N.A. Artem'eva, V. Shuvalov, Shock Waves 5 (1996) 359 https://doi.org/10.1007/BF02434011
[6] J. Borovička, B. Spurný, W. P, K. P, C. P, D., Nature 503 (2013) 235 https://doi.org/10.1038/nature12671
[7] Jenniskens, Adv. Space Res. 39 (2007) 491 https://doi.org/10.1016/j.asr.2007.03.040
[8] B. Mason, Geochimica et Cosmochimica Acta, 30 (1966) 23 https://doi.org/10.1016/0016-7037(66)90089-5
[9] A. A. Berezhnoy, Icarus 300 (2018) 210 https://doi.org/10.1016/j.icarus.2017.08.034
[10] A.A. Berezhnoy, J. Borovička, Icarus 210 (2010) 150 https://doi.org/10.1016/j.icarus.2010.06.036
[11] J. Borovička, P. Spurný, Icarus 121 (1996) 484 https://doi.org/10.1006/icar.1996.0104
[12] A.F. Jaleel, H.R.H. Ahmed, Exp Theor. NANOTECHNOLOGY 10 (2026) 37 https://doi.org/10.56053/10.1.37
[13] AM, H. TK, G. AJ, D. M, Exp Theor. NANOTECHNOLOGY 10 (2026) 131 https://doi.org/10.56053/10.1.131
[14] P. Agrawal, P.M. Jenniskens, E. Stern, J. Arnold, Y.K. Chen, Aerodyn. Meas. Technol. Ground Test. Conf. 1 (2018) 4284 https://doi.org/10.2514/6.2018-4284
[15] H. R. Ali, W. I. Yaseen, Exp. Theor. NANOTECHNOLOGY. 9 (2025) 209 https://doi.org/10.56053/9.S.209
[16] Z.J. Jaffer, S.N. Mazhir, M.K. Khalaf, H. aMS, J. Phys. Conf. Ser. 1829 (2021) 1 10.1088/1742-6596/1829/1/012010
[17] K. Yamada, Y. Yamamoto, K. Tomioka, ChemInform 36 (2025) 17 https://doi.org/10.1002/chin.200517257
[18] A. F. Serov, A. D. Nazarov, V. N. Mamonov, V. I. Terekhov, Applied Energy 251 (2019) 113362 https://doi.org/10.1016/j.apenergy.2019.113362
[19] A. Birch, P. Elliott, S. Mukerjee, T. Rajagopalan, T. Seshadri, S. Varadarajan, Australian Journal of Chemistry 8 (1955) 409 https://doi.org/10.1071/ch9550409
[20] W.I. Yaseen, A.F. Ahmed, D.A. Al-Shakarchi, F.A.-H. Mutlak, Appl. Phys. A 128 (2022) 148 https://doi.org/10.1007/s00339-022-05301-w
[21] C. Aragón, J.A. Aguilera, Spectrochim. Acta Part B At. Spectrosc. 63 (2008) 893 https://doi.org/10.1016/j.sab.2008.05.010
[22] M. J. White, F. Southwood, K. Huddlestone, First Language 1 (2022) 01427 https://doi.org/10.1177/01427237221112064
[23] H.O. Hussein, W.I. Yaseen, Iraqi J. Sci. 1 (2024) 29. https://doi.org/10.24996/ijs.2024.65.5.43
[24] W.I. Yaseen, A.K. Abd, Iraqi J. Sci. (2024) 5026 https://doi.org/10.24996/ijs.2024.65.9.19
[25] N. Konjević, F. Lesage JR, W.L. Wiese, J. Phys. Chem. Ref. Data 31 (2002) 819 https://doi.org/10.1002/chin.200517257

[26] Wedyan G. Nassif, Nadia M. Abed, Ruaa M. Ibrahim, Amal Jaafar Salim Al-Azawee, Osama T. Al-Iaai, Experimental and Theoretical NANOTECHNOLOGY 10 (2026) 153 https://doi.org/10.56053/10.1.153
[27] K.A. Aadim, A.A. Hussain, W.I. Yaseen, Iraqi J. Phys. 13 (2015) 76 https://doi.org/10.30723/ijp.v13i27.266
[28] H.R. Humud, Iraqi J. Phys. 15 (2017) 142 https://doi.org/10.30723/ijp.v15i35.63
[29] F. Akin, O. Arikan, Journal of Applied Polymer Science 142 (2025) 35 https://doi.org/10.1002/app.57380
[30] Abdulameer Hassan Abdulameer, S. Z. Hussein, Iraqi Journal of Science 55 (2023) 2669 https://doi.org/10.24996/ijs.2023.64.6.2
[31] I. Alshalal, H. M. I. Al-Zuhairi, A. A. Abtan, M. Rasheed, M. K. Asmail. J. Mech. Behav. Mater. 32 (2023) 1 https://doi.org/10.1515/jmbm-2022-0280
[32] M. Sellam, M. Rasheed, S. Azizi, T. Saidani. Ceram. Int. 50 (2024) 20917 https://doi.org/10.1016/j.ceramint.2024.03.094
[33] O. Alabdali, S. Shihab, M. Rasheed, T. Rashid. 3rd inter. Scient. conf. alkafeel univ. (ISCKU 2021) (2022) https://doi.org/10.1063/5.0066860
[34] M. Rasheed, O. Alabdali, S. Shihab, A. Rashid, T. Rashid, J. Phys.: Conf. Ser. 1999 (2021) 012078 https://doi.org/10.1088/1742-6596/1999/1/012078
[35] N. Assoudi et al. Opt. Quant. Electron. 54 (2022) 9 https://doi.org/10.1007/s11082-022-03927-x
[36] R. Jalal, S. Shihab, M.A. Alhadi, M. Rasheed, J. Phys.: Conf. Ser. 1660 (2020) 012090 https://doi.org/10.1088/1742-6596/1660/1/012090
[37] S. Shihab, M. Rasheed, O. Alabdali, A.A. Abdulrahman, J. Phys.: Conf. Ser. 1879 (2021) 022120. https://doi.org/10.1088/1742-6596/1879/2/022120
[38] A. Keziz, M. Heraiz, M. RASHEED, A. Oueslati. Mater Chem. Phys. 325 (2024) 129757 https://doi.org/10.1016/j.matchemphys.2024.129757
[39] D. Kherifi, A. Keziz, M. Rasheed, A. Oueslati. Ceram. Int. 50 (2024) 30175 https://doi.org/10.1016/j.ceramint.2024.05.317
[40] A. Jaber, M. Ismael, T. Rashid, M. A. Sarhan, M. Rasheed, I. M. Sala. Eureka: Phys. Eng. 4 (2023) 29 https://doi.org/10.21303/2461-4262.2023.002770
[41] T. Rashid, M. M. Mokji, M. Rasheed. J. Optics 33 (2024) 57 https://doi.org/10.1007/s12596-024-02080-w
[42] H. K. Aity, E. Dhahri, M. Rasheed. Ceram. Int. 50 (2024) 54666 https://doi.org/10.1016/j.ceramint.2024.10.324
[43] M. Rasheed, S. Shihab, O. Alabdali, A. Rashid, T. Rashid, J. Phys.: Conf. Ser. 1999 (2021) 012077 https://doi.org/10.1088/1742-6596/1999/1/012077
[44] M. Rasheed, M. Nuhad Al-Darraji, S. Shihab, A. Rashid, T. Rashid. J. Phys.: Conf. Ser. 1963 (2021) 012058 https://doi.org/10.1088/1742-6596/1963/1/012058
[45] A. Keziz, M. Heraiz, F. Sahnoune, M. Rasheed, Ceram. Int. 49 (2023) 32989 https://doi.org/10.1016/j.ceramint.2023.07.275
[46] E. Kadri, K. Dhahri, R. Barillé, M. Rasheed. Phase Transi. 94 (2021) 65 https://doi.org/10.1080/01411594.2020.1832224
[47] D. Bouras, M. Rasheed, Opt. Quantum Electron. 54 (2022) 12 https://doi.org/10.1007/s11082-022-04161-1
[48] A. Zubaidi, L.M. Asaad, I. Alshalal, M. Rasheed, J. Mech. Behav. Mater. 32 (2023) 1 https://doi.org/10.1515/jmbm-2022-0302
[49] M. Rasheed et al., J. Phys.: Conf. Ser. 1999 (2021) 012080 https://doi.org/10.1088/1742-6596/1999/1/012080
[50] M. Rasheed, M.N. Al-Darraji, S. Shihab, A. Rashid, T. Rashid, J. Phys.: Conf. Ser. 1963 (2021) 012059 https://doi.org/10.1088/1742-6596/1963/1/012059

[51] M. Enneffatia, M. Rasheed, B. Louati, K. Guidara, S. Shihab, R. Barillé, J. Phys.: Conf. Ser. 1795 (2021) 012050 https://doi.org/10.1088/1742-6596/1795/1/012050
[52] M. Rasheed, O.Y. Mohammed, S. Shihab, A. Al-Adili, J. Phys.: Conf. Ser. 1795 (2021) 012043 https://doi.org/10.1088/1742-6596/1795/1/012043
[53] A.H. Ali, A.S. Jaber, M.T. Yaseen, M. Rasheed, O. Bazighifan, T.A. Nofal, Complexity 2022 (2022) 1 https://doi.org/10.1155/2022/9367638
[54] M. Rasheed, et al., J. Adv. Biotechnol. Exp. Ther. 6 (2023) 495 https://doi.org/10.5455/jabet.2023.d144
[55] M. Rasheed, I. Alshalal, A.A. Ashed, M.A. Sarhan, A.S. Jaber, Indones. J. Electr. Eng. Comput. Sci. 33 (2024) 653 https://doi.org/10.11591/ijeecs.v33.i1.pp653-660
[56] I.M. Mohammed, M. Rasheed, AIP Conf. Proc. 3321 (2025) 020026 https://doi.org/10.1063/5.0289719
[57] F. Boudou, A. Belakredar, A. Berkane, M. Rasheed. Not. Sci. Biol. 17 (2025) 12183 https://doi.org/10.55779/nsb17212183
[58] F. Boudou, et al., Not. Sci. Biol. 17(3) (2025) 12593 https://doi.org/10.55779/nsb17312593
[59] F. Boudou, A. Guendouzi, A. Belkredar. M. Rasheed, Not. Sci. Biol. 16 (2024) 13837 https://doi.org/10.55779/nsb16211837
[60] R.S. Mahmood et al. J. Mech. Behav. Mater. 34 (2025) 1 https://doi.org/10.1515/jmbm-2025-0040
[61] T. Rashid, M.M. Mokji, M. Rasheed, J. Mech. Behav. Mater. 34 (2025) 77 https://doi.org/10.1515/jmbm-2025-0074
[62] M. Rasheed, M. N. Mohammedali, F. A. Sadiq, M. A. Sarhan, T. Saidani. J. Optics (New Delhi. Print) (2024) https://doi.org/10.1007/s12596-024-01928-5
[63] A.J. Hussein, M.N. Al-Darraji, M. Rasheed, M.A. Sarhan, IOP Conf. Ser.: Earth Environ. Sci. 1262 (2023) 022007 https://doi.org/ 10.1088/1755-1315/1262/2/022007
[64] A.J. Hussein, M.N. Al-Darraji, M. Rasheed, M.A. Sarhan, IOP Conf. Ser.: Earth Environ. Sci. 1262 (2023) 022005 https://doi.org/10.1088/1755-1315/1262/2/022005
[65] T. Saidani, M. Rasheed, I. Alshalal, A.A. Rashed, M.A. Sarhan, R. Barillé, Res. Eng. Struct. Mater. 10 (2024) 743 http://dx.doi.org/10.17515/resm2023.21ma0922rs
[66] M. A. Sarhan, S. Shihab, B. E. Kashem, M. Rasheed, J. Phy.: Conf. Ser., 1879 (2021) 022122 https://doi.org/10.1088/1742-6596/1879/2/022122
[67] M. Rasheed, O. Alabdali, S. Shihab, J. Phy.: Conf. Ser. 1879 (2021) 032120 https://doi.org/10.1088/1742-6596/1879/3/032120
[68] M. Rasheed, R. Barillé, J. Non-Cryst. Solids., 476 (2017) 1 https://doi.org/10.1016/j.jnoncrysol.2017.04.027
[69] M. Rasheed, R. Barillé, Opt. Quantum Electron. 49 (2017) 99 https://doi.org/10.1007/s11082-017-1030-7
[70] F. Dkhilalli, S. M. Borchani, M. Rasheed, R. Barille, K. Guidara, M. Megdiche, J. Mater. Sci. Mater. Electron, 29 (2018) 6297 https://doi.org/10.1007/s10854-018-8609-z
[71] A. Boumezoued, K. Guergouri, Régis Barillé, Rechem Djamil, Mourad Zaabat, M. Rasheed, J. Alloys Compd. 791 (2019) 550 https://doi.org/10.1016/j.jallcom.2019.03.251
[72] N. Ben Azaza et al., Opt. Mater., 96 (2019) 109328 https://doi.org/10.1016/j.optmat.2019.109328
[73] Areej Adnan Hateef, Essebti Dhahri, M. Rasheed, Habiba Kadhim, Z. Abbas, N. Hassan, Physics and Chemistry of Solid State, 25 (2024) 801 https://doi.org/10.15330/pcss.25.4.801-810
[74] M. Rasheed, SuhaShihab, O. Alabdali, H. H. Hassan, J. Phys. Conf. Ser., 1879 (2021) 032113 https://doi.org/10.1088/1742-6596/1879/3/032113
[75] H. K. Aity, M. Rasheed, E. Dhahri, A. A. Hateef, T. Saidani, Journal of Materials Science, 61 (2026) 6226 https://doi.org/10.1007/s10853-026-12241-w

[76] T. Saidani, S. Mokhtari, M. Rasheed, H. Lahmar, M. Trari, Journal of the Indian Chemical Society, 103 (2026) 102499 https://doi.org/10.1016/j.jics.2026.102499
[77] M. RASHEED, A. Khaleefah, Materials Chemistry and Physics, 353 (2026) 132112 https://doi.org/10.1016/j.matchemphys.2026.132112
[78] S. S. Batros, M. Rasheed, H. K. Aity, A. A. Hatef, T. Saidani, Materials Chemistry and Physics, 355 (2026) 132243 https://doi.org/10.1016/j.matchemphys.2026.132243
[79] A. Raghdi, M. Heraiz, M. Rasheed, A. Keziz, Journal of the Indian Chemical Society, 101 (2024) 101413 https://doi.org/10.1016/j.jics.2024.101413
[80] A. I. A. Ali, M. RASHEED, Experimental and Theoretical NANOTECHNOLOGY 10 (2026) 277 https://doi.org/10.56053/10.s.277
[81] A. Khaleefah, M. RASHEED, Experimental and Theoretical NANOTECHNOLOGY 10 (2026) 289 https://doi.org/10.56053/10.s.289
[82] Z. S. Ahmed, M. RASHEED, H. S. Ahmed, Experimental and Theoretical NANOTECHNOLOGY 10 (2026) 329 https://doi.org/10.56053/10.s.329
[83] Z. S. Ahmed, M. RASHEED, H. S. Ahmed, Experimental and Theoretical NANOTECHNOLOGY 10 (2026) 343 https://doi.org/10.56053/10.s.343
[84] A. I. A. Ali, M. RASHEED, Experimental and Theoretical NANOTECHNOLOGY 10 (2026) 239 https://doi.org/10.56053/10.s.239